DELAYED MODEL FOR THE TRANSMISSION AND CONTROL OF COVID-19 WITH FANGCANG SHELTER HOSPITALS[*]

GUIHONG FAN[†], JUAN LI[‡], JACQUES BÉLAIR[§], AND HUAIPING ZHU[¶]

Abstract. The ongoing coronavirus disease 2019 (COVID-19) pandemic poses a huge threat to global public health. Motivated by China's experience of using Fangcang shelter hospitals (FSHs) to successfully combat the epidemic in its initial stages, we present a two-stage delay model considering the average waiting time of patients' admission to study the impact of hospital beds and centralized quarantine on mitigating and controlling of the outbreak. We compute the basic reproduction number in terms of the hospital resources and perform a sensitivity analysis of the average waiting times of patients before admission to the hospitals. We conclude that, while designated hospitals save lives in severely infected individuals, the FSHs played a key role in mitigating and eventually curbing the epidemic. We also quantified some key epidemiological indicators, such as the final size of infections and deaths, the peak height and its timing, and the maximum occupation of beds in FSHs. Our study suggests that, for a jurisdiction (region or country) still struggling with COVID-19, when possible, it is essential to increase testing capacity and use a centralized quarantine to massively reduce the severity and magnitude of the epidemic that follows.

Key words. COVID-19, transmission, Fangcang shelter hospital beds, delay, basic reproduction number, control

MSC codes. 37N25, 37N30, 39A60

DOI. 10.1137/21M146154X

1. Introduction. Coronavirus disease 2019 (COVID-19), caused by severe acute respiratory syndrome coronavirus 2 (SARS-CoV-2) [42], was first detected in Wuhan in the Hubei Province of China in December 2019 and has spread worldwide since [16, 39]; outbreaks have been reported in 219 countries or territories [43]. By October, 2021, there were 236.60 million confirmed cases and 4.83 million deaths which were reported to World Health Organization (WHO) [41]. Though vaccination has become available, the pandemic remains a serious global health problem: as of the last week of September 2021, more than 3 million weekly new cases were reported to WHO, as well as 54,000 weekly deaths [41]. The most severely affected countries include the United States, India, and Brazil [34].

[†]Department of Mathematics, Columbus State University, Columbus, GA 31907 USA (fan_guihong@columbus.state.edu).

[‡]School of Computer Science and Technology (School of Artificial Intelligence), Zhejiang Sci-Tech University, Hangzhou 310018, Zhejiang, PR China, and LAMPS and Center for Diseases Modeling CDM, Department of Mathematics and Statistics, York University, Toronto M3J 1P3, ON, Canada (lijuanjuan0120@163.com).

[§]Département de Mathématiques et de Statistique and Centre de Recherches Mathématiques, Université de Montréal, Montréal H3C 3J7, QC, Canada (jacques.belair@umontreal.ca).

[¶]LAMPS and Center for Diseases Modeling CDM, Department of Mathematics and Statistics, York University, Toronto M3J 1P3, ON, Canada (huaiping@mathstatyorku.edu).

SARS-CoV-2 causes only mild, flu-like symptoms in the majority of infected cases. But some patients may develop severe symptoms, like trouble breathing and persistent pain or pressure in the chest, so they need emergency medical care, like ventilator support [15]. Most people infected can recover at home, and there is currently no specific treatment available for COVID-19 [14]. Severe illness can occur in as many as 14% of patients contracting the virus. The overall death rate due to infection is estimated at 2.3%, while the death rate among older adults (70 years or older) is higher at between 8%–14.8% [44].

Before the availability of vaccines, the mainstay of treatments for COVID-19 was supportive care and optimized symptomatic treatment [17]. Prevention and nonpharmaceutical interventions (NPIs) are the keys to pandemic control [32]. The common NPIs include social distancing, mask-wearing, good personal hygiene, self-isolation, school closures, banning of public events, and curfew. Among these interventions, city lockdown has proven to help slow down the spread of COVID-19 in a region or a country [33]. However, the epidemic continued in most countries well after WHO declared the COVID-19 as a global pandemic on March 11, 2020 [38].

Aside from China, most countries where the pandemic was most successfully kept under control, such as Singapore, Japan, and the Republic of Korea, had been following the principles of early detection, testing, early quarantine, and treatment, based on the experience and lessons from China's successful battle with the virus [2]. These principles are the main content of the recommendations provided by WHO after its experts finished a fact-finding mission in China [38].

The mutation of the coronavirus, and the ensuing circulation of its variants, has added a level of difficulty to the control of the disease. Since the current treatments or vaccines are developed based on the earlier strain of the virus, this can maybe offer only limited protection against the new variants [18]. Currently, Canada is dealing with the variant-driven fourth wave of the coronavirus pandemic [27]. Several European countries (France, Germany, Poland, etc.) have also battled the fourth wave and reintroduced lockdowns to curb the third wave of infections by implementing stricter measures to last several weeks at least [7]. Though these countries also strictly implemented NPIs, including lockdown, social distancing, face-mask–wearing, and community and school closures, the pandemic still prevales.

To reduce the rapid spread of the COVID-19, the city of Wuhan, China, decided on a city lockdown on January 23, 2020, and travel bans were also announced for several nearby cities [25]. Wuhan also took different actions to alleviate the shortage in medical resources, as thousands of confirmed cases overwhelmed the city's health care system. Several hospitals were assigned to be designated hospitals (DHs) for COVID-19, which made the number of open beds for coronavirus infections 11,500 as of February 2 [35]. The launch of Huoshenshan Hospital (opened on February 3) and Leishenshan Hospital (opened on February 8) added 2,600 more beds in the city [35]. However, the number of daily confirmed cases still kept increasing and did not show any sign of weakening.

On February 5, 2020, the first Fangcang shelter hospitals (FSHs) started to accept patients for massive group isolation of all confirmed mild infections. A dozen venues, such as gymnasiums and conference centers, were converted to sprawling medical wards, referred to as FSHs later [5].

While DHs were used for severe patients, FSHs were used for mild infections in order to isolate them massively. In addition, Wuhan also implemented a close contact tracing and testing strategy. In February 2020, Wuhan community workers began a door-to-door campaign to identify anyone with exposure to confirmed cases or exhibiting symptoms themselves. Then the confirmed cases (mild or asymptomatic)

were sent to FSHs immediately for group quarantine. After the implementation of FSHs, the FSHs were full even though new beds kept adding to the system until February 22, 2020, which was when it was observed that the pandemic was mitigated when the FSHs started to have the first vacant beds available to wait for new confirmed cases. By March 16, 2020 the number of infected patients was kept under double digits for days, and thus the COVID-19 was successfully controlled. Use of central quarantine in FSHs rather than sending the patients to recuperate at home, where they often infected family members, is now credited for bringing the outbreak in Wuhan under control [26]. It was contact tracing and testing and, in particular, the increasing number of FSH beds allowing the massive group quarantine that helped curb the epidemics in Wuhan [22].

The fluctuation of the epidemics before and after reopening in different stages indicates that lockdown helps mitigate the spread of the disease but not enough to suppress and prevent a pendemic. Other NPIs are needed to assist with disease control. The current pandemic of the virus in many other countries also indicates that home quarantine is useful but insufficient for pandemic control.

There are two types of time delays that play a significant role in the spread of COVID-19. One type is associated with the virus evolution, like latency period [23], and the other type is related to medical resources or human interventions [22, 28]. Several COVID-19 models consider the latency period of the virus [23]. They modeled the latency period by introducing an exposed class (E) of infected individuals, who are not infectious yet. Liu et al. [23] considered an alternative delay differential equations model with a latent time delay in which they estimated the latency period in the dynamics of COVID-19. Dell'Anna [9] studied a single functional delay differential equation with a time-dependent infection rate in which the author assumes that an infected individual has a fixed period to transmit the virus.

The second type of delay is associated with human interventions, such as contact tracing, testing, and diagnosis or treatment. Kretzschmar et al. [19] considered a stochastic mathematical model with two time delays, one of which is a testing delay, of the order of up to 7 days, and the other is a tracing delay, of up to 3 days. Rong et al. [28] established a compartmental susceptible-exposed-infectious-removed model with a delay in diagnosis considered. They divided infected individuals into two different groups: one is in a resource-rich setting which provides for timely diagnosis, while the other is in a resource-poor setting and with a longer diagnostic waiting time.

Compared to the these delays, the waiting time for the confirmed infectious individuals to be admitted into DHs or FSHs is crucial in preventing further infections. If the number of FSH beds is not enough to keep up with the needs, a longer waiting time is required for the confirmed cases to be group isolated. Therefore, in this paper, we develop a compartment model incorporating the delays of average waiting time (in days) of the confirmed infectious individuals before they were admitted into either DHs or FSHs.

A number of modeling studies have considered the impact of hospital beds in extending the time needed to recover [1, 29, 30]. However, none considered the time delays due to the lack of available beds to admit infectious individuals. We study the dynamics of the delay models and explore how the two delays and the number of hospital beds in DHs ad FSHs affect the transmission dynamics of the virus. We also estimate the minimum number of beds in FSHs needed for curbing the epidemic.

This paper is organized as follows: section 2 is devoted to modeling. We consider two delayed models with and without FSHs to compare the role of FSHs in subsection 2.1. In subsection 2.2, we establish the positivity and boundedness of the proposed

models. In section 3, we calculate the basic reproduction number and estimate the minimum number of hospital beds needed for controlling the epidemic. We define the elasticity of the basic reproduction number to quantify the impact of waiting times. We introduce the contribution index to identify the relative contribution of either hospital in the control of the disease. In section 7, we fit the data of clinical cases in Wuhan to our model to estimate some critical parameters related to disease transmission. Then we use these estimates to run simulations with or without FSHs, which allow us to compare and contrast the impact of waiting time for the different hospitals. Our results can provide some insightful information for public health to prepare and manage the hospital beds for better control of the ongoing epidemic. Discussion and suggestions are in section 8.

2. Compartmental models with delays of waiting time.

2.1. Model formation. The 2020 pandemic of COVID-19 in Wuhan can be divided into two phases: Phase I occurred before FSHs were built (before February 5), and Phase II took place after FSHs were put into use. Inspired by the idea in [22], we adapt a susceptible (S)–exposed (E)–asymptomatic (A)–infectious (prodromal phase, I_1)–infectious (with symptoms I_2)–hospitalized–recovered framework for COVID-19 dynamics (see Figure 1 for the flowchart). Our exposed class (E) represents patients in the latent period during which patients carry the virus but do not spread the virus yet. The class A represents the group of people who do not develop any symptoms at all during their whole infection process, while class I_1 represents the group of people who do not shows symptoms for a temporary time period but will develops symptoms later and get into either I_2 or I_m and I_s classes with symptoms. We propose two delayed models: one with FSHs and the other without FSHs. Since both delays represent the waiting time for using hospital facilities, the delay is zero if there

(a) Without FSHs

(b) With FSHs
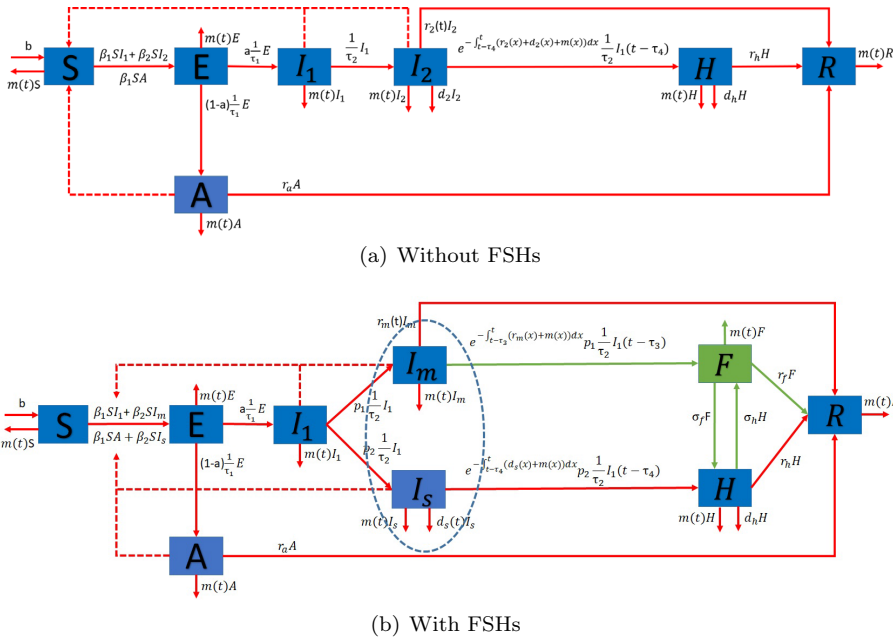
Fig. 1. *Flow diagram for the transmission of COVID-19.*

TABLE 1
Description of all parameters in the model (2.9).

Parameter	Description	Mean value	Resource
β_1	Average infection rate of the susceptible by infectious individuals without symptoms (1/day)	$1.3581\text{e--}07^{noFSH}$, $2.5584\text{e--}09^{FSH}$	Estimated
β_2	Average infection rate of the susceptible by infectious symptomatic individuals who are not hospitalized yet (1/day)	$1.4462\text{e--}08^{noFSH}$, $2.0433\text{e--}10^{FSH}$	Estimated
τ_1	Average time spent in the class E (day)	4	[22]
τ_2	Average time spent in the class I_1 (day)	3	[22]
τ_3	Average waiting time of mildly infected patients from onset of symptoms to FSHs (day)	3.0219	Estimated
τ_4	Average waiting time of severely infected patients from onset of symptoms to DHs with or without FSHs (day)	6.9428^{noFSH}, 4.1722^{FSH}	Estimated
p_1	Average fraction of patients admitted into FSHs (dimensionless)	0.823	[49]
p_2	Average fraction of patients admitted into DHs (dimensionless)	0.177	[49]
r_a	Average recovery rate of the inapparent infected (1/day)	1/7	[10]
r_m	Average recovery rate of the mildly infected individuals outside the hospital (1/day)	$5.6962\text{e--}02$	Estimated
r_f	Average recovery rate of patients in FSHs (1/day)	$1.5820\text{e--}02^{noFSH}$, $2.6922\text{e--}02^{FSH}$	Estimated
r_h	Average recovery rate of patients in DHs (1/day)	$7.855\text{e--}03^{noFSH}$, $1.3463\text{e--}02^{FSH}$	Estimated
a	Average fraction of infections that become symptomatic (dimensionless)	0.9530	[22]
σ_f	Average transfer rate of patients from FSHs to DHs (1/day)	0.035^a	[4]
σ_h	Average transfer rate of patients from DHs to FSHs (1/day)	$6.3993\text{e--}02$	Estimated
d_s	Average disease-induced death rate of the severely infected individuals outside the hospital (1/day)	$1.8621\text{e--}02$	Estimated
d_h	Average disease-induced death rate of patients in DHs (1/day)	$4.7655\text{e--}03$	Estimated
b	Average number of births per day (individual/day)	393^b	[46]
m	Average natural death rate of human (1/day)	0.013^c	[46]
r_2	Average recovery rate of patients with symptoms outside hospitals without FSHs (1/day)	0.0133	[22]
d_2	Average disease-induced death rate of patients with symptoms outside hospitals without FSHs (1/day)	0.0306	[22]

[a]From the reporting [4], the conversion rate from mild to severe was $2\% - 5\%$ here we take the average 0.035.
[b]Parameter b is calculated by $\frac{1.1212 \times 10^7 \times 0.01280}{365}$, where 1.1212×10^7 is the total resident population and 0.01280 is the proportion of new births in Wuhan in 2019.
[c]Parameter m is the reciprocal of the average lifetime of humans in Wuhan, where the average lifetime is about 76.95 years in 2019.

are enough hospital beds to treat the severe cases or to group isolate the mild cases. Otherwise, the delay is positive when the average waiting time is long due to a limited number of hospital beds. All variables and parameters appearing in the models are listed in Tables 1 and 2. Initial data are given in (2.10), and practical initial values for parameter estimation are listed in Table 2.

TABLE 2
Description of all variables in the model (2.9).

Variable	Description	Value	Resource
$S(0)$	Initial susceptible population (individual)	1.1212e+07	[46]
$E(0)$	Initial exposed population (individual)	1.4001e+03	Estimated
$A(0)$	Initial inapparent infected population (individual)	5.0675e+02	Estimated
$I_1(0)$	Initial infectious population without symptoms (individual)	1.0242e+03	Estimated
$I_m(T_1)$	Initial infectious population with mild symptoms (individual)	$0.823I_2(T_1)^a$	Estimated
$I_s(T_1)$	Initial the infectious population with severe symptoms (individual)	$0.177I_2(T_1)$	Estimated
$F(0)$	Initial infected population in FSHs (individual)	3,025	[48]
$H(0)$	Initial infected population in DHs (individual)	441^b	Calculated
$R(0)$	Initial recovered population due to COVID-19 (individual)	31	[48]
$I_2(0)$	Initial infectious population with symptoms (individual)	9.9485e+02	Estimated

^{a}Here T_1 denotes the time February 5, 2020, when FSHs were put into service.
^{b}According to the policy "Receive all patients" implemented in China, $H(0)$ is calculated by the cumulative confirmed cases (495)-(Cumulative recoveries (31)+Cumulative deaths (23)) on January 23, 2020.

Delay differential equation model without FSHs.
To control the spread of COVID-19 in January 2020, Wuhan initiated the policy of "receive as many patients as possible and treat as many as possible for the confirmed COVID-19 cases" [6]. However, at the early stage of the epidemic control, due to the lack of knowledge about the coronavirus, the limitation in testing resources, and the slow turnover time, for a the vast majority of patients, the period from infection to diagnosis or treatment would take a certain amount of time [40, 51].

Let $I_1(t)$ represent the patients without symptoms who will develop symptoms later and $I_2(t)$ be the symptomatic patients with mild or severe symptoms who are waiting for hospital beds. Before FSHs were put into use, we assume the average waiting time τ_4 (from clinical symptom onset to being treated in DHs) of patients in the I_2 class is an integer number of days, rounded up to 1 if the waiting time is less than one day. The patients hospitalized at time t are those who had clinical symptoms at time $t-\tau_4$. The patients in I_2 with clinical symptoms are only expected to go through a removal process at a rate of $r_2(x)+d_2(x)+m(x)$, where $r_2(x)$, $d_2(x)$, $m(x)$ represent recovery rate, disease-induced death rate, and natural death rate, respectively, during the period $x \in (t-\tau_4, t)$. As discussed in Thieme [36] and Zhao [50], we can write

$$(2.1) \qquad I_2(t) = \int_{t-\tau_4}^{t} e^{-\int_s^t (r_2(x)+d_2(x)+m(x))dx} \frac{1}{\tau_2} I_1(s)ds.$$

When $\tau_4 = 0$, we have $I_2 = 0$, which means there are no cases accumulated in the I_2 class. Alternatively, the infected individuals enter the hospital as soon as they are confirmed before showing clinical symptoms.

Taking the derivative of $I_2(t)$ with respect to t gives

$$(2.2) \qquad I_2{}'(t) = \frac{1}{\tau_2}I_1 - e^{-\int_{t-\tau_4}^{t}(r_2(x)+d_2(t)+m(x))dx} \frac{1}{\tau_2}I_1(t-\tau_4)$$
$$- r_2(t)I_2 - d_2(t)I_2 - m(t)I_2.$$

Considering the delayed effect of admission, the flow of patients into the DHs at time t from I_2 class is $\frac{1}{\tau_2}I_1(t - \tau_4)$. However, some patients may have been removed (recovered or died) during the waiting process. Here, $e^{-\int_s^t (r_2(x)+d_2(x)+m(x))dx}$ represents the probability of patients in I_1, who show symptoms at time s, but remain in waiting for hospital admission until time t. This probabiliy helps exclude the portion of patients who either recovered or died before time t. Then the actual rate of patients who are hospitalized successfully into DHs at time t is given by $e^{-\int_{t-\tau_4}^t (r_2(x)+d_2(x)+m(x))dx}\frac{1}{\tau_2}I_1(t - \tau_4)$.

By Figure 1 (top) and the above argument, we have the delayed model without FSHs

$$(2.3) \quad \begin{cases} S' = b - \beta_1 S(A + I_1) - \beta_2 SI_2 - m(t)S, \\[2mm] E' = \beta_1 S(A + I_1) + \beta_2 SI_2 - \dfrac{1}{\tau_1}E - m(t)E, \\[2mm] A' = (1-a)\dfrac{1}{\tau_1}E - r_a A - m(t)A, \\[2mm] I_1' = a\dfrac{1}{\tau_1}E - \dfrac{1}{\tau_2}I_1 - m(t)I_1, \\[2mm] I_2' = \dfrac{1}{\tau_2}I_1 - e^{-\int_{t-\tau_4}^t (r_2(x)+d_2(x)+m(x))dx}\dfrac{1}{\tau_2}I_1(t - \tau_4) \\[2mm] \qquad - r_2(t)I_2 - d_2(t)I_2 - m(t)I_2, \\[2mm] H' = e^{-\int_{t-\tau_4}^t (r_2(x)+d_2(x)+m(x))dx}\dfrac{1}{\tau_2}I_1(t - \tau_4) - r_h H - d_h H - m(t)H, \\[2mm] R' = r_a A + r_2(t)I_2 + r_h H - m(t)R. \end{cases}$$

Delay differential equations model with FSHs.
When the lockdown started in Wuhan, a large number of DHs were made available for severe cases, and the epidemic was expected to improve in about two weeks. However, the daily number of new confirmed cases kept increasing, and the epidemic situation became even worse. The capacity of DHs was insufficient. A large number of mildly infected patients were asked to quarantine at home. The Wuhan authority started to realize that household transmission can lead to more infections; hence the massive tracing, testing, and group isolating of the mild and asymptomatic infections became crucial.

According to the "FSH management rules" formulated by the medical treatment group of Wuhan New Pneumonia Prevention and Control Headquarters, FSHs in principle treated mildly infected patients who had been diagnosed and were not accepted by DHs [6]. Here the key for the epidemic prevention was to treat the confirmed cases in hospitals (FSHs) instead of at home and to carry out centralized treatment and isolation to avoid the contact with family and social circle members. In particular, mildly infected patients having strong mobility presented a greater risk of infection. Therefore, in order to expand the capacity and achieve the centralized isolation and treatment of mildly infected patients, the Wuhan municipal government started the construction of FSHs in February 2020. Starting February 5, 2020, FSHs started to accept and isolate the confirmed mild and asymptomatic infectious individuals [47].

To capture the special role of FSHs in preventing and controlling further infections, we add the patients in FSHs as a separate state variable (denoted by $F(t)$) in the model and further divide the patients in compartment $I_2(t)$ into two subgroups: mildly infected patients who are waiting for FSHs at time t (denoted by $I_m(t)$) and severely infected ones who are waiting for DHs at time t (denoted by $I_s(t)$). Due to the limitations of the number of beds in both DHs and FSHs, we assume that the

average waiting times for patients in $I_m(t)$ and $I_s(t)$ before admission are τ_3 and τ_4 days, respectively.

It is assumed that mildly infected patients will be transferred to DHs immediately once they develop severe symptoms. Thus, the infected individuals in FSHs will either recover or be transferred to DHs for treatment but not die of infection in FSHs. Analogously, during the waiting time, patients in $I_m(t)$ are only removed due to recovery or natural death with a removal rate denoted by $r_m(x) + m(x)$ for $x \in (t - \tau_3, t)$. Similar to the expression of $I_2(t)$, we can write $I_m(t)$ as

$$(2.4) \qquad I_m(t) = \int_{t-\tau_3}^{t} e^{-\int_s^t (r_m(x)+m(x))dx} p_1 \frac{1}{\tau_2} I_1(s)ds,$$

and its derivative of $I_m(t)$ with respect to t yields

$$(2.5) \qquad \begin{aligned} I_m{}'(t) = {} & p_1 \frac{1}{\tau_2} I_1 - e^{-\int_{t-\tau_3}^t (r_m(x)+m(x))dx} p_1 \frac{1}{\tau_2} I_1(t-\tau_3) \\ & - r_m(t)I_m - m(t)I_m. \end{aligned}$$

As emphasized in the introduction, severe illness among COVID-19 patients can occur in as many as 14% of infections. The overall death rate of infection is 2.3%, while the death rate among older adults (70 years or older) is 8%–14.8% [44]. Severe cases are admitted to DHs for treatment, and they either recover or die of infection. It is worth noting that all COVID-19 infection–induced deaths occur in DHs. Similarly, we define $I_s(t)$ as

$$(2.6) \qquad I_s(t) = \int_{t-\tau_4}^{t} e^{-\int_s^t (d_s(x)+m(x))dx} p_2 \frac{1}{\tau_2} I_1(s)ds$$

and compute

$$(2.7) \qquad \begin{aligned} I_s{}'(t) = {} & p_2 \frac{1}{\tau_2} I_1 - e^{-\int_{t-\tau_4}^t (d_s(x)+m(x))dx} p_2 \frac{1}{\tau_2} I_1(t-\tau_4) \\ & - d_s(t)I_s - m(t)I_s, \end{aligned}$$

where d_s denotes the disease-induced death rate of severe infections due to COVID-19.

Considering the special role of FSHs (see Figure 1 (bottom)), model (2.3) becomes

$$\begin{cases} S' = b - \beta_1 S(A+I_1) - \beta_2 S(I_m+I_s) - m(t)S, \\[4pt] E' = \beta_1 S(A+I_1) + \beta_2 S(I_m+I_s) - \dfrac{1}{\tau_1}E - m(t)E, \\[4pt] A' = (1-a)\dfrac{1}{\tau_1}E - r_a A - m(t)A, \\[4pt] I_1{}' = a\dfrac{1}{\tau_1}E - \dfrac{1}{\tau_2}I_1 - m(t)I_1, \\[4pt] I_m{}' = p_1\dfrac{1}{\tau_2}I_1 - e^{-\int_{t-\tau_3}^t (r_m(x)+m(x))dx} p_1\dfrac{1}{\tau_2}I_1(t-\tau_3) - r_m(t)I_m - m(t)I_m, \\[4pt] I_s{}' = p_2\dfrac{1}{\tau_2}I_1 - e^{-\int_{t-\tau_4}^t (d_s(x)+m(x))dx} p_2\dfrac{1}{\tau_2}I_1(t-\tau_4) - d_s(t)I_s - m(t)I_s, \\[4pt] F' = e^{-\int_{t-\tau_3}^t (r_m(x)+m(x))dx} p_1\dfrac{1}{\tau_2}I_1(t-\tau_3) - \sigma_f F + \sigma_h H - r_f F - m(t)F, \\[4pt] H' = e^{-\int_{t-\tau_4}^t (d_s(x)+m(x))dx} p_2\dfrac{1}{\tau_2}I_1(t-\tau_4) + \sigma_f F - \sigma_h H - r_h H - d_h H - m(t)H, \\[4pt] R' = r_a A + r_m(t)I_m + r_f F + r_h H - m(t)R. \end{cases}$$

The focus of this paper is the investigation of the impact of FSHs and the waiting time delays (which depends on the availability of FSH beds) on the development of the epidemic. Though the number of hospital beds in both DHs and FSHs changes daily, in order to study how the public health (the number of beds available and health personnel) and other medical resources facilitate the disease control in both hospitals, as in [22], we assume that the numbers of doctors, health care personnel, and all other essential medical resources are recruited and coordinated so that the waiting times τ_3 and τ_4 remain constant. Then we obtain the following two models with constant coefficients:

$$(2.8) \quad \begin{cases} S' = b - \beta_1 S(A + I_1) - \beta_2 S I_2 - mS, \\[4pt] E' = \beta_1 S(A + I_1) + \beta_2 S I_2 - \dfrac{1}{\tau_1}E - mE, \\[4pt] A' = (1-a)\dfrac{1}{\tau_1}E - r_a A - mA, \\[4pt] I_1' = a\dfrac{1}{\tau_1}E - \dfrac{1}{\tau_2}I_1 - mI_1, \\[4pt] I_2' = \dfrac{1}{\tau_2}I_1 - e^{-(r_2+d_2+m)\tau_4}\dfrac{1}{\tau_2}I_1(t-\tau_4) - r_2 I_2 - d_2 I_2 - mI_2, \\[4pt] H' = e^{-(r_2+d_2+m)\tau_4}\dfrac{1}{\tau_2}I_1(t-\tau_4) - r_h H - d_h H - mH, \\[4pt] R' = r_a A + r_2 I_2 + r_h H - mR \end{cases}$$

and

$$(2.9) \quad \begin{cases} S' = b - \beta_1 S(A + I_1) - \beta_2 S(I_m + I_s) - mS, \\[4pt] E' = \beta_1 S(A + I_1) + \beta_2 S(I_m + I_s) - \dfrac{1}{\tau_1}E - mE, \\[4pt] A' = (1-a)\dfrac{1}{\tau_1}E - r_a A - mA, \\[4pt] I_1' = a\dfrac{1}{\tau_1}E - \dfrac{1}{\tau_2}I_1 - mI_1, \\[4pt] I_m' = p_1\dfrac{1}{\tau_2}I_1 - e^{-(r_m+m)\tau_3}p_1\dfrac{1}{\tau_2}I_1(t-\tau_3) - r_m I_m - mI_m, \\[4pt] I_s' = p_2\dfrac{1}{\tau_2}I_1 - e^{-(d_s+m)\tau_4}p_2\dfrac{1}{\tau_2}I_1(t-\tau_4) - d_s I_s - mI_s, \\[4pt] F' = e^{-(r_m+m)\tau_3}p_1\dfrac{1}{\tau_2}I_1(t-\tau_3) - \sigma_f F + \sigma_h H - r_f F - mF, \\[4pt] H' = e^{-(d_s+m)\tau_4}p_2\dfrac{1}{\tau_2}I_1(t-\tau_4) + \sigma_f F - \sigma_h H - r_h H - d_h H - mH, \\[4pt] R' = r_a A + r_m I_m + r_f F + r_h H - mR. \end{cases}$$

In all the above models, all parameters are positive, and their descriptions are summarized in Table 1. All state variables and constant initial values are given in Table 2, and the initial conditions of the delayed variables can be found in (2.10).

In this paper, we analyze both models, one corresponding to Phase I of pandemic control before FSHs were constructed and the other one for Phase II after the FSHs started to accept mildly infected patients (on February 5, 2020). We will use both models to estimate the basic reproduction numbers and compare the risk of the pandemic with or without FSHs. In addition, we estimate and present the threshold of the minimum number of beds needed in FSHs for successfully controlling the epidemic.

2.2. The positivity and boundedness of solutions. In this section, we prove the positivity and boundedness of both systems (2.8) and (2.9) following a method similar to the proof of Lemma 2.1 in [21]. Because of this similarity, we only include the detailed proof for system (2.9), the proof for system (2.8) following, mutatis mutandis.

To establish the well-posedness of the system (2.9), we choose the phase space $\bar{\mathcal{C}} := \mathcal{C}([-\hat{\tau}, 0], \mathbb{R}^9)$, where $\hat{\tau} = \max\{\tau_3, \tau_4\}$. Define $\bar{\mathcal{C}}^+ := \mathcal{C}([-\hat{\tau}, 0], \mathbb{R}^9_+)$. Then $(\bar{\mathcal{C}}, \bar{\mathcal{C}}^+)$ is an ordered Banach space equipped with the maximum norm. For any continuous function $x : [-\hat{\tau}, \sigma) \to \mathbb{R}^9_+$ with $\sigma > 0$, we define $x_t \in \bar{\mathcal{C}}$ as $x_t(\theta) = x(t + \theta)$ for any $\theta \in [-\hat{\tau}, 0]$ for any $t \in [0, \sigma)$. Define a feasible region

$$(2.10) \qquad \Omega_\delta = \left\{ \phi \in \bar{\mathcal{C}}^+ : \sum_{j=1}^{9} \phi_i(s) \geq \delta, \phi_5(0) = \int_{-\tau_3}^{0} e^{(r_m+m)s} p_1 \frac{1}{\tau_3} I_1(s) ds, \right.$$

$$\left. \phi_6(0) = \int_{-\tau_4}^{0} e^{(d_s+m)s} p_2 \frac{1}{\tau_4} I_1(s) ds, \ \phi_j(0) \geq 0 \text{ for other } j \right\}$$

for any given $\delta \in (0, \frac{b}{d_s+d_h+m})$.

THEOREM 2.1. *For system (2.9) with the initial conditions $\phi \in \Omega_\delta$, there exists a unique nonnegative solution $x(t, \phi)$ with $x_0 = \phi$ for all $t \geq 0$. All solutions are nonnegative, bounded, and finally located in the region of Ω_δ for sufficiently large t.*

Proof. For any $\phi \in \Omega_\delta$, we define $\bar{f}(t, \phi) = (f_1(t, \phi), f_2(t, \phi), f_3(t, \phi), \ldots, f_9(t, \phi))$, where

$$f_1(t, \phi) = b - \beta_1 \phi_1(0)(\phi_3(0) + \phi_4(0)) - \beta_2 \phi_1(0)(\phi_5(0) + \phi_6(0)) - m\phi_1(0),$$

$$f_2(t, \phi) = \beta_1 \phi_1(0)(\phi_3(0) + \phi_4(0)) + \beta_2 \phi_1(0)(\phi_5(0) + \phi_6(0)) - \frac{1}{\tau_1}\phi_2(0) - m\phi_2(0),$$

$$f_3(t, \phi) = (1 - a)\frac{1}{\tau_1}\phi_2(0) - r_a \phi_3(0) - m\phi_3(0),$$

$$f_4(t, \phi) = a\frac{1}{\tau_1}\phi_2(0) - \frac{1}{\tau_2}\phi_4(0) - m\phi_4(0),$$

$$f_5(t, \phi) = p_1 \frac{1}{\tau_2}\phi_4(0) - e^{-(r_m+m)\tau_3} p_1 \frac{1}{\tau_2}\phi_4(-\tau_3) - r_m \phi_5(0) - m\phi_5(0),$$

$$f_6(t, \phi) = p_2 \frac{1}{\tau_2}\phi_4(0) - e^{-(d_s+m)\tau_4} p_2 \frac{1}{\tau_2}\phi_4(-\tau_4) - d_s \phi_6(0) - m\phi_6(0),$$

$$f_7(t, \phi) = e^{-(r_m+m)\tau_3} p_1 \frac{1}{\tau_2}\phi_4(-\tau_3) - \sigma_f \phi_7(0) + \sigma_h \phi_8(0) - r_f \phi_7(0) - m\phi_7(0),$$

$$f_8(t, \phi) = e^{-(d_s+m)\tau_4} p_2 \frac{1}{\tau_2}\phi_4(-\tau_4) + \sigma_f \phi_7(0) - \sigma_h \phi_8(0) - r_h \phi_8(0) - d_h \phi_8(0) - m\phi_8(0),$$

$$f_9(t, \phi) = r_a \phi_3(0) + r_m \phi_5(0) + r_f \phi_7(0) + r_h \phi_8(0) - m\phi_9(0).$$

Since $\bar{f}(t, \phi)$ is Lipschitz continuous in $(t, \phi) \in \mathbb{R}_+ \times \Omega_\delta$, by Theorems 2.2.1 and 2.2.3 in Hale and Verduyn Lunel [13], system (2.9) has a unique solution $x(t, \phi)$ with $x_0 = \phi$ on its maximum interval $[0, \sigma)$ of existence.

With the compatibility conditions in Ω_δ, the differential equations for I_m and I_s in system (2.9) are equivalent to the integral equations (2.4) and (2.6), respectively. Therefore, $x_5(t) = I_m(t) \geq 0$ and $x_6(t) = I_s(t) \geq 0$ for any $t \in [0, t_0]$ whenever $x_4(t) = I_1(t) \geq 0$ for $t \in [0, t_0] \subset [0, \sigma)$.

Consider an initial condition $\phi = (\phi_1, \phi_2, \phi_3, \ldots, \phi_9) \in \Omega_\delta$. If $\phi_i(0) = 0$ for some $i = \{1, 2, 3, 4, 7, 8, 9\}$, then $f_i(t, \phi) \geq 0$. By Theorem 5.2.1 in Smith [31], it follows that the unique solution $x_i(t, \phi) \geq 0$ for any $t \in [0, \sigma_\phi)$. From the integrals of I_m and I_s,

we have $x_5(t) = I_m \geq 0$ and $x_6(t) = I_s \geq 0$ for any $t \in [0, \sigma_\phi)$. Therefore, for any $\phi \in \Omega_\delta$, the unique solution $x(t, \phi)$ of the system (2.9) with $x_0 = \phi$ is nonnegative for any $t \in [0, \sigma_\phi)$.

Let $N(t) = S(t) + E(t) + A(t) + I_1(t) + I_m(t) + I_s(t) + F(t) + H(t) + R(t)$. We have $N'(t) = b - d_s I_s(t) - d_h H(t) - mN(t) \geq b - (d_s + d_h + m)N(t)$ since $0 \leq I_s(t), H(t) \leq N(t)$. Note that the linear equation $y' = b - (d_s + d_h + m)y(t)$ has a globally stable equilibrium $\frac{b}{d_s + d_h + m}$. For any $0 < \delta < b/(d_s + d_h + m)$, we have $y'|_{y=\delta} = b - (d_s + d_h + m)\delta > 0$. If $y(0) \geq \delta$, then $y(t) \geq \delta$ for any $t \geq 0$. By the comparison principle, $N(t) \geq \delta$ if $N(0) \geq \delta$. This implies $x_t(\phi) \in \Omega_\delta$ for any $t \in [0, \sigma_\phi)$.

Alternatively we have $N'(t) = b - d_s I_s - d_h H - mN(t) \leq b - mN(t)$ for any $t \in [0, \sigma_\phi)$. It follows that $N(t)$ is bounded on $[0, \sigma_\phi)$. Hence, Theorem 2.3.1 in Hale and Verduyn Lunel [13] implies that $\sigma_\phi = \infty$. Therefore, solutions are ultimately bounded. Note that $N'(t) < 0$ whenever $N(t) > b/m$. This implies that solutions are uniformly bounded. □

3. Equilibria and the basic reproduction number R_0. The basic reproduction number R_0 is the number of secondary infections caused by one infected individual in a fully susceptible population during its entire infectious period. The R_0 is a critical indicator to evaluate the transmission power of a disease. In this section, we compute the basic reproduction numbers of both systems (2.8) and (2.9) by applying the method in [37] for compartmental systems with time delays.

It is easy to see that systems (2.8) and (2.9) always have a disease-free equilibrium $E^0_{noFSH}(S^0, 0, 0, 0, 0, 0, 0)$ or $E^0_{FSH}(S^0, 0, 0, 0, 0, 0, 0, 0, 0)$, respectively, with $S^0 = b/m$.

We first calculate R_0 for the system (2.9) with two delays. The infected compartments include E, A, I_1, I_m, I_s, F, and H. Here, we only consider the infected classes E, A, I_1, I_m, and I_s since the F and H classes do not participate in virus transmission. We have the nonnegative matrices $\tilde{F}$ describing the derivatives of the nonlinear terms (in the equation of E) evaluated at the disease-free equilibrium E^0_{FSH},

$$\tilde{F} = \begin{bmatrix} 0 & \beta_1 S^0 & \beta_1 S^0 & \beta_2 S^0 & \beta_2 S^0 \\ 0 & 0 & 0 & 0 & 0 \\ 0 & 0 & 0 & 0 & 0 \\ 0 & 0 & 0 & 0 & 0 \\ 0 & 0 & 0 & 0 & 0 \end{bmatrix}.$$

We also obtain a cooperative matrix $V = V_1 + V_2 + V_3$ showing the derivatives of the outflow terms at E^0_{FSH}:

$$V_1 = \begin{bmatrix} 0 & 0 & 0 & 0 & 0 \\ 0 & 0 & 0 & 0 & 0 \\ 0 & 0 & 0 & 0 & 0 \\ 0 & 0 & -e^{-(r_m+m)\tau_3}p_1/\tau_2 & 0 & 0 \\ 0 & 0 & 0 & 0 & 0 \end{bmatrix}, \quad V_2 = \begin{bmatrix} 0 & 0 & 0 & 0 & 0 \\ 0 & 0 & 0 & 0 & 0 \\ 0 & 0 & 0 & 0 & 0 \\ 0 & 0 & 0 & 0 & 0 \\ 0 & 0 & -e^{-(d_s+m)\tau_4}p_2/\tau_2 & 0 & 0 \end{bmatrix},$$

$$V_3 = \begin{bmatrix} -(1/\tau_1 + m) & 0 & 0 & 0 & 0 \\ (1-a)/\tau_1 & -(r_a + m) & 0 & 0 & \\ a/\tau_1 & 0 & -(1/\tau_2 + m) & 0 & 0 \\ 0 & 0 & p_1/\tau_2 & -(r_m + m) & 0 \\ 0 & 0 & p_2/\tau_2 & 0 & -(d_s + m) \end{bmatrix}.$$

It follows that $V(\phi) = V_1\phi(-\tau_3) + V_2\phi(-\tau_4) + V_3\phi(0)$, where $\phi \in C([-\tau_m, 0], R^5)$, which is the continuous Banach space equipped with the maximum norm with $\tau_m =$

$\max\{\tau_3, \tau_4\}$. The basic reproduction number of system (2.9) is determined by the spectral radius of $\rho(-\tilde{F}V^{-1})$, where $\tilde{F}$ is positive and $V = V_1 + V_2 + V_3$ is an invertible quasi-positive matrix (page 189 in [37]) since

$$\frac{p_1}{\tau_2}[1 - e^{-(r_m+m)\tau_3}] > 0, \qquad \frac{p_2}{\tau_2}[1 - e^{-(d_s+m)\tau_4}] > 0.$$

We have

$$\mathrm{R}_0^{FSH} = \rho(-\tilde{F}V^{-1}) = QS^0,$$

where $S^0 = b/m$ and

$$Q = \frac{\beta_1}{(1+m\tau_1)}\left[\frac{(1-a)}{(r_a+m)} + \frac{a\tau_2}{(1+m\tau_2)}\right]$$
$$+ \frac{\beta_2 a}{(1+m\tau_1)(1+m\tau_2)}\left[\frac{p_1(1 - e^{-(r_m+m)\tau_3})}{(r_m+m)} + \frac{p_2(1 - e^{-(d_s+m)\tau_4})}{(d_s+m)}\right].$$

Similarly, we get R_0^{noFSH} for system (2.8) as

$$\mathrm{R}_0^{noFSH} = \tilde{Q}S^0$$

with

$$\tilde{Q} = \frac{\beta_1}{(1+m\tau_1)}\left[\frac{(1-a)}{(r_a+m)} + \frac{a\tau_2}{(1+m\tau_2)}\right] + \frac{\beta_2 a}{(1+m\tau_1)(1+m\tau_2)}\left[\frac{p_1(1 - e^{-(r_2+d_2+m)\tau_h})}{(r_2+d_2+m)}\right].$$

We can obtain directly the above expression of R_0^{FSH} based on the existence of an endemic equilibrium for system (2.9). At any equilibrium $(\tilde{S}, \tilde{E}, \tilde{A}, \tilde{I}_1, \tilde{I}_m, \tilde{I}_s, \tilde{F}, \tilde{H}, \tilde{R})$ of (2.9), we have

(3.1)
$$\begin{cases}
\tilde{E} = \dfrac{\tau_1}{1+m\tau_1}(b - m\tilde{S}), \\[2mm]
\tilde{A} = \dfrac{(1-a)\frac{1}{\tau_1}}{r_a+m}\tilde{E} = \dfrac{1-a}{(r_a+m)(1+m\tau_1)}(b - m\tilde{S}), \\[2mm]
\tilde{I}_1 = \dfrac{a\frac{1}{\tau_1}}{\frac{1}{\tau_2}+m}\tilde{E} = \dfrac{a\tau_2}{\tau_1(1+m\tau_2)}\tilde{E} = \dfrac{a\tau_2}{(1+m\tau_1)(1+m\tau_2)}(b - m\tilde{S}), \\[2mm]
\tilde{I}_m = \dfrac{p_1(1 - e^{-(r_m+m)\tau_3})}{\tau_2(r_m+m)}\tilde{I}_1 = \dfrac{p_1(1 - e^{-(r_m+m)\tau_3})a}{(r_m+m)(1+m\tau_1)(1+m\tau_2)}(b - m\tilde{S}), \\[2mm]
\tilde{I}_s = \dfrac{p_2(1 - e^{-(d_s+m)\tau_4})}{\tau_2(d_s+m)}\tilde{I}_1 = \dfrac{p_2(1 - e^{-(d_s+m)\tau_4})a}{(d_s+m)(1+m\tau_1)(1+m\tau_2)}(b - m\tilde{S}), \\[2mm]
\tilde{F} = \dfrac{p_1(\sigma_h+r_h+d_h+m)e^{-(r_m+m)\tau_3} + p_2\sigma_h e^{-(d_s+m)\tau_4}}{\tau_2(\sigma_f+r_f+m)(\sigma_h+r_h+d_h+m) - \tau_2\sigma_f\sigma_h}\tilde{I}_1, \\[2mm]
\tilde{H} = \dfrac{p_2 e^{-(d_s+m)\tau_4}(\sigma_f+r_f+m) + p_1\sigma_f e^{-(r_m+m)\tau_3}}{\tau_2(\sigma_f+r_f+m)(\sigma_h+r_h+d_h+m) - \tau_2\sigma_f\sigma_h}\tilde{I}_1, \\[2mm]
\tilde{R} = \dfrac{r_a\tilde{A} + r_m\tilde{I}_m + r_f\tilde{F} + r_h\tilde{H}}{m}.
\end{cases}$$

By the first equation in system (2.9), we have

$$b - \left[\beta_1(\tilde{A} + \tilde{I}_1) + \beta_2(\tilde{I}_m + \tilde{I}_s) + m\right]\tilde{S} = 0.$$

Substituting $\tilde{E}, \tilde{A}, \tilde{I}_1, \tilde{I}_m, \tilde{I}_s$ into the above equation yields

$$b - (Qb + m)\tilde{S} + Qm(\tilde{S})^2 = 0.$$

Solving for $\tilde{S}$ gives

$$\tilde{S} = \frac{1}{Q} \qquad \text{or} \qquad \tilde{S} = \frac{b}{m}.$$

Substituting $\tilde{S} = b/m$ into (3.1), we obtain $E_{FSH}^0 = (S^0, 0, 0, 0, 0, 0, 0, 0, 0)$ with $S^0 = b/m$. Substituting $\tilde{S} = 1/Q$ into (3.1) gives $E_{FSH}^*(S^*, E^*, A^*, I_1^*, I_m^*, I_s^*, F^*, H^*, R^*)$ with $S^* = 1/Q$. The endemic equilibrium exists provided $1/Q < b/m$ so that the exposed class $E^* > 0$, where $1/Q < b/m$ is equivalent to $R_0^{FSH} > 1$. From a biological interpretation, when the ratio of natural birth and natural death is larger than the threshold value $1/Q$, the disease will persist.

4. Global stability of disease-free equilibrium. Regarding the global stability of equilibria, we have the following theorem.

THEOREM 4.1. *If $R_0^{FSH} < 1$, the disease-free equilibrium E_0 is globally attractive for system* (2.9) *with the initial conditions in Ω_δ.*

Proof. The total population $N = S + E + A + I_1 + I_m + I_s + F + H + R$ satisfies

(4.1) $$N' = b - mN - d_s I_s - d_h H.$$

By Lemma 2.1, we have $I_s(t) \geq 0$ and $H(t) \geq 0$. Therefore,

(4.2) $$N' \leq b - mN.$$

Since equation $y' = b - my$ has a global attractor $y = b/m$, by the comparison principle, we have $N(t) < b/m + \epsilon$ for small $\epsilon > 0$ and sufficiently large t. Therefore

(4.3) $$0 < S(t) < N(t) < b/m + \epsilon$$

for sufficiently large t.

If $R_0^{FSH} < 1$, we substitute $S = \frac{b}{m} + \epsilon = S^0 + \epsilon$ into (2.9) and obtain the following perturbed linear system:

(4.4)
$$
\begin{cases}
E' = \beta_1(S^0 + \epsilon)(A + I_1) + \beta_2(S^0 + \epsilon)(I_m + I_s) - \dfrac{1}{\tau_1}E - mE, \\[2mm]
A' = (1 - a)\dfrac{1}{\tau_1}E(t) - r_a A - mA, \\[2mm]
I_1' = a\dfrac{1}{\tau_1}E(t) - \dfrac{1}{\tau_2}I_1 - mI_1, \\[2mm]
I_m' = p_1\dfrac{1}{\tau_2}I_1 - e^{-(r_m + m)\tau_3}p_1\dfrac{1}{\tau_2}I_1(t - \tau_3) - r_m I_m - mI_m, \\[2mm]
I_s' = p_2\dfrac{1}{\tau_2}I_1 - e^{-(d_s + m)\tau_4}p_2\dfrac{1}{\tau_2}I_1(t - \tau_4) - d_s I_s - mI_s.
\end{cases}
$$

Similarly we can define $R_0^{FSH}(\epsilon)$ as we did in section 3. Define $R_0^{FSH}(\epsilon) = r(-\tilde{F}_\epsilon V^{-1})$. We have $\lim_{\epsilon \to 0} R_0^{FSH}(\epsilon) = R_0^{FSH} < 1$, where

$$
\tilde{F}_\epsilon = \begin{bmatrix}
0 & \beta_1(S^0 + \epsilon) & \beta_1(S^0 + \epsilon) & \beta_2(S^0 + \epsilon) & \beta_2(S^0 + \epsilon) \\
0 & 0 & 0 & 0 & 0 \\
0 & 0 & 0 & 0 & 0 \\
0 & 0 & 0 & 0 & 0 \\
0 & 0 & 0 & 0 & 0
\end{bmatrix}.
$$

Therefore, we can fix ϵ small enough so that $R_0^{FSH}(\epsilon) < (1 + R_0^{FSH})/2 := \sigma$ which is less than 1.

Since V is a quasi-positive matrix, by Theorem 2.4 [37, page 190], V is resolvent positive. In addition, the eigenvalues of matrix V are $\lambda = -(\frac{1}{\tau_1}+m), -(\gamma_a+m), -(\frac{1}{\tau_2}+m)$, or $-(\gamma_m+m)$, and $-(d_s+m)$. Therefore the spectral bound $s(V) = \max\{-(\frac{1}{\tau_1}+m), -(\gamma_a+m), -(\frac{1}{\tau_2}+m), -(\gamma_m+m), -(d_s+m)\} < 0$, which is the largest real part of eigenvalues of matrix V.

Define matrix $A = F_\epsilon + V$. Since F_ϵ is a positive matrix, we have that matrix A is quasi-positive and thus resolvent positive by Theorem 2.4 [37, page 190]. Since matrix V is resolvent positive and $s(V) < 0$, by Theorem 3.5 [37, page 191], spectral bound $s(A)$ has the same sign as $\rho(-F_\epsilon V^{-1}) - 1 = R_0^{FSH}(\epsilon) - 1$, which is less than zero for small $\epsilon > 0$. Hence, the spectral bound $s(A)$ is less than zero.

The characteristic equations of matrix A are

$$(4.5) \qquad P(\lambda, \tau) + \frac{p_1}{\tau_2}[1 - e^{-(r_m+m)\tau_3}]Q_1(\lambda, \tau) + \frac{p_2}{\tau_2}[1 - e^{-(d_s+m)\tau_4}]Q_2(\lambda, \tau) = 0,$$

where $P(\lambda, \tau)$ is a fourth order polynomial of λ and $Q_i(\lambda, \tau)$ is a third order polynomial of λ ($i = 1, 2$). Since $s(A) < 0$, all eigenvalues λ_i of A have a negative real part ($i = 1, 2, 3, 4$). Choose $-s(A)/2 < \delta < 0$ so that $\mathrm{Re}\lambda_i < \delta$.
Accordingly the characteristic equation of the following delayed equation (4.4) at $(0, 0, 0, 0, 0)$ is

$$P(\lambda, \tau) + \frac{p_1}{\tau_2}Q_1(\lambda, \tau) + \frac{p_2}{\tau_2}Q_2(\lambda, \tau)$$

$$(4.6) \qquad - \left\{\frac{p_1}{\tau_2}e^{-(r_m+m)\tau_3}e^{-\lambda\tau_3}Q_1(\lambda, \tau) + \frac{p_2}{\tau_2}e^{-(d_s+m)\tau_4}e^{-\lambda\tau_4}Q_2(\lambda, \tau)\right\} = 0.$$

Let $l \in \{\lambda \in \mathcal{C} | \mathrm{Re}(\lambda) > -\delta\}$ be a simple closed curve enclosed λ_1, λ_2, λ_3, and λ_4. Then we can choose δ small enough so that the characteristic matrix of the delayed equation is

$$\begin{bmatrix} -(1/\tau_1 + m) - \lambda & \beta_1 S^0 & \beta_1 S^0 & \beta_2 S^0 & \beta_2 S^0 \\ (1-a)/\tau_1 & -(r_a+m)-\lambda & 0 & 0 & 0 \\ a/\tau_1 & 0 & -(1/\tau_2+m)-\lambda & 0 & 0 \\ 0 & 0 & p_1/\tau_2[1-e^{-(r_m+m)\tau_3}e^{-\lambda\tau_3}] & -(r_m+m)-\lambda & 0 \\ 0 & 0 & p_2/\tau_2[1-e^{-(d_s+m)\tau_4}e^{-\lambda\tau_4}] & 0 & -(d_s+m)-\lambda \end{bmatrix}.$$

By Hal [31, page 91], the equilibrium point $(0, 0, 0, 0, 0)$ of system (4.4) is asymptotically stable if $s(A) < 0$. By (4.3), any solution $(E(t), A(t), I_1(t), I_m(t), I_s(t))$ of (2.9) is nonnegative and satisfies

$$(4.7) \qquad \begin{cases} E' \le \beta_1(S^0 + \epsilon)(A + I_1) + \beta_2(S^0 + \epsilon)(I_m + I_s) - \dfrac{1}{\tau_1}E - mE, \\[2mm] A' \le (1-a)\dfrac{1}{\tau_1}E(t) - r_a A - mA, \\[2mm] I_1' \le \dfrac{1}{\tau_1}E(t) - \dfrac{1}{\tau_2}I_1 - mI_1, \\[2mm] I_m' \le p_1\dfrac{1}{\tau_2}I_1 - e^{-(r_m+m)\tau_3}p_1\dfrac{1}{\tau_2}I_1(t-\tau_3) - r_m I_m - mI_m, \\[2mm] I_s' \le p_2\dfrac{1}{\tau_2}I_1 - e^{-(d_s+m)\tau_4}p_2\dfrac{1}{\tau_2}I_1(t-\tau_4) - d_s I_s - mI_s \end{cases}$$

for sufficiently large t. By the comparison theorem of delay differential equations (Theorem 5.1.1 in [31]), we have $\lim_{t\to\infty} E(t), A(t), I_1(t), I_m(t), I_s(t) \to 0$. From $\lim_{t\to\infty} I_1(t) \to 0$, we can show that $\lim_{t\to\infty} F(t), H(t), R(t) \to 0$. Therefore the boundary equilibrium is $E_{FSH}^0(S^0, 0, 0, 0, 0, 0, 0, 0, 0)$ is globally asymptotically stable.   □

5. Local stability of endemic equilibrium E_{FSH}^*. The characteristic equation $\Delta(\lambda) = |M| = |A| * |B|$ at endemic equilibrium E_{FSH}^* is given by the determinant of the following matrix:

$$M = \begin{bmatrix} A & 0 \\ C & B \end{bmatrix},$$

where A, B, C are block matrix with

$$C = \begin{bmatrix} 0 & 0 & 0 & e^{-(\gamma_m + m)\tau_3} \frac{p_1}{\tau_2} e^{-\lambda\tau_3} & 0 & 0 \\ 0 & 0 & 0 & e^{-(d_s + m)\tau_4} \frac{p_2}{\tau_2} e^{-\lambda\tau_4} & 0 & 0 \end{bmatrix},$$

$$B = \begin{bmatrix} -\sigma_f - \gamma_f - m - \lambda & \sigma_h \\ \sigma_f & -\sigma_h - \gamma_h - d_h - m - \lambda \end{bmatrix},$$

$$A = \begin{bmatrix} a_{11} - \lambda & 0 & a_{13} & a_{13} & a_{13} & a_{13} \\ a_{21} & a_{22} - \lambda & -a_{13} & -a_{13} & -a_{13} & -a_{13} \\ 0 & a_{32} & a_{33} - \lambda & 0 & 0 & 0 \\ 0 & a_{42} & 0 & a_{44} - \lambda & 0 & 0 \\ 0 & 0 & \frac{p_1}{\tau_2}\left(1 - e^{-(\gamma_m + m + \lambda)\tau_3}\right) & 0 & a_{55} - \lambda & 0 \\ 0 & 0 & \frac{p_2}{\tau_2}\left(1 - e^{-(d_s + m + \lambda)\tau_4}\right) & 0 & 0 & a_{66} - \lambda \end{bmatrix}$$

with

$$a_{11} = -\beta_1(A^* + I_1^*) - \beta_2(I_m^* + I_s^*) - m, \qquad a_{13} = -\beta_1 S^*,$$

$$a_{21} = \beta_1(A^* + I_1^*) + \beta_2(I_m^* + I_s^*), \qquad a_{22} = -\frac{1}{\tau_1} - m,$$

$$a_{32} = \frac{1 - a}{\tau_1}, \qquad a_{33} = -\gamma_a - m,$$

$$a_{42} = \frac{a}{\tau_1}, \qquad a_{44} = -\frac{1}{\tau_2} - m,$$

$$a_{55} = -\gamma_m - m, \qquad a_{66} = -d_s - m.$$

Note that

$$\Delta(\lambda, \tau) = |M| = |A| * |B|.$$

From $|B| = 0$, we have

$$(\lambda + \sigma_f + m + \gamma_f)(\lambda + \gamma_h + d_h + m + \sigma_h) - \sigma_h \sigma_f = 0,$$

which has two negative real roots. The stability of the interior equilibrium is determined by the roots of $|A| = 0$ which are

$$
\begin{aligned}
|A| = {}& (a_{11} - \lambda)(a_{22} - \lambda)(a_{33} - \lambda)(a_{44} - \lambda)(a_{55} - \lambda)(a_{66} - \lambda) \\
& - (m + \lambda)a_{13}a_{32}(a_{44} - \lambda)(a_{55} - \lambda)(a_{66} - \lambda) \\
& - (m + \lambda)a_{13}a_{42}(a_{33} - \lambda)(a_{66} - \lambda)(a_{55} - \lambda) \\
& + (m + \lambda)a_{13}a_{32}(a_{44} - \lambda)(a_{55} - \lambda)\frac{p_2}{\tau_2}\left[1 - e^{-(d_s + m + \lambda)\tau_4}\right] \\
& + (m + \lambda)a_{13}a_{32}(a_{44} - \lambda)(a_{66} - \lambda)\frac{p_1}{\tau_2}\left[1 - e^{-(\gamma_m + m + \lambda)\tau_3}\right].
\end{aligned}
$$

We make the following assumptions:

(H$_1$) Assume $\beta_1 S^* < \frac{1}{2}|a_{11} + m|$.

(H$_2$) Assume $|a_{13}a_{32}|[\frac{p_2}{\tau_2}(1 + e^{(m - d_s - m)\tau_4}) + \frac{p_1}{\tau_2}(1 + e^{-\gamma_m \tau_3})] < \frac{1}{2}|a_{11} + m||a_{22} + m||a_{33} + m|$.

THEOREM 5.1. *If conditions* (H$_1$) *and* (H$_2$) *hold, the characteristic equation evaluated at* E^*_{FSH} *has no roots with real part larger than* $-m$. *Hence, the interior equilibrium* E^*_{FSH} *is locally asymptotically stable.*

Proof. We use a proof by contradiction. Assume that the characteristic equation has a root $\lambda = \alpha + i\beta$ with $\alpha > -m$. Then we have

$$
\begin{aligned}
|Q(\lambda, \tau)| := {}& \Big|(m + \lambda)a_{13}a_{32}(a_{44} - \lambda)(a_{55} - \lambda)(a_{66} - \lambda) \\
& + (m + \lambda)a_{13}a_{42}(a_{33} - \lambda)(a_{66} - \lambda)(a_{55} - \lambda) \\
& - (m + \lambda)a_{13}a_{32}(a_{44} - \lambda)(a_{55} - \lambda)\frac{p_2}{\tau_2}\left[1 - e^{-(d_s + m + \lambda)\tau_4}\right] \\
& - (m + \lambda)a_{13}a_{32}(a_{44} - \lambda)(a_{66} - \lambda)\frac{p_1}{\tau_2}\left[1 - e^{-(\gamma_m + m + \lambda)\tau_3}\right]\Big|
\end{aligned}
$$

(5.1)
$$
= |(a_{11} - \lambda)(a_{22} - \lambda)(a_{33} - \lambda)(a_{44} - \lambda)(a_{55} - \lambda)(a_{66} - \lambda)| := |P(\lambda, \tau)|.
$$

We do an estimation for the left-hand side:

$$
\begin{aligned}
|Q(\lambda, \tau)| < {}& |(m + \lambda)a_{13}a_{32}(a_{44} - \lambda)(a_{55} - \lambda)(a_{66} - \lambda)| \\
& + |(m + \lambda)a_{13}a_{42}(a_{33} - \lambda)(a_{66} - \lambda)(a_{55} - \lambda)| \\
& + \left|(m + \lambda)a_{13}a_{32}(a_{44} - \lambda)(a_{55} - \lambda)\frac{p_2}{\tau_2}\left[1 - e^{-(d_s + m + \lambda)\tau_4}\right]\right| \\
& + \left|(m + \lambda)a_{13}a_{32}(a_{44} - \lambda)(a_{66} - \lambda)\frac{p_1}{\tau_2}\left[1 - e^{-(\gamma_m + m + \lambda)\tau_3}\right]\right|.
\end{aligned}
$$

Note that $-\gamma_a - m < -m < \alpha$; we have

$$
\begin{aligned}
|m + \lambda| &= |\lambda - (-m)| = |\alpha + i\beta - (-m)| = |(\alpha - (-m)) + i\beta| \\
&< |\alpha - (-\gamma_a - m) + i\beta| = |\lambda - a_{33}|.
\end{aligned}
$$

Similarly $|m + \lambda| < |\lambda - a_{44}|$, $|m + \lambda| < |\lambda - a_{55}|$, and $|m + \lambda| < |\lambda - a_{66}|$:

$$
\begin{aligned}
|Q(\lambda, \tau)| \\
< {}& |(a_{33} - \lambda)(a_{44} - \lambda)(a_{55} - \lambda)(a_{66} - \lambda)||a_{13}(a_{32} + a_{42})| \\
& + |(a_{44} - \lambda)(a_{55} - \lambda)(a_{66} - \lambda)|a_{13}a_{32}|\left[\frac{p_2}{\tau_2}(1 + e^{-d_s \tau_4}) + \frac{p_1}{\tau_2}(1 + e^{-\gamma_m \tau_3})\right]
\end{aligned}
$$

$$= |(a_{33} - \lambda)(a_{44} - \lambda)(a_{55} - \lambda)(a_{66} - \lambda)| \left[\beta_1 S^* \frac{1}{\tau_1} \right]$$
$$+ |(a_{44} - \lambda)(a_{55} - \lambda)(a_{66} - \lambda)| a_{13} a_{32} \left[\frac{p_2}{\tau_2} (1 + e^{-d_s \tau_4}) + \frac{p_1}{\tau_2} (1 + e^{-\gamma_m \tau_3}) \right].$$

From assumption (H_1), we have

$$\beta_1 S^* \frac{1}{\tau_1} < \frac{1}{2} |a_{11} + m||a_{22} + m| < \frac{1}{2} |a_{11} - \lambda||a_{22} - \lambda|.$$

From assumption (H_2), we have

$$|a_{13} a_{32}| \left[\frac{p_2}{\tau_2} (1 + e^{-d_s \tau_4}) + \frac{p_1}{\tau_2} (1 + e^{-\gamma_m \tau_3}) \right]$$
$$< \frac{1}{2} |a_{11} + m||a_{22} + m||a_{33} + m| < \frac{1}{2} |a_{11} - \lambda||a_{22} - \lambda||a_{33} - \lambda|.$$

Therefore, we have

$$|Q(\lambda, \tau)| < \frac{1}{2} |(a_{11} - \lambda)(a_{22} - \lambda)(a_{33} - \lambda)(a_{44} - \lambda)(a_{55} - \lambda)(a_{66} - \lambda)|$$
$$+ \frac{1}{2} |(a_{11} - \lambda)(a_{22} - \lambda)(a_{33} - \lambda)(a_{44} - \lambda)(a_{55} - \lambda)(a_{66} - \lambda)|$$
$$= |P(\lambda, \tau)|,$$

which contradicts (5.1). Therefore, under assumptions (H_1) and (H_2), $\sup\{\text{Re}\lambda : \Delta(\lambda, \tau) \leq -m$. By Theorem 4.1 in [20, page 25], the interior equilibrium E^*_{FSH} is locally asymptotically stable.   □

6. Risk assessment and the number of hospital beds needed in FSHs.

6.1. Elasticity of R_0^{FSH}. Recall that τ_3 and τ_4 are two key parameters reflecting the investment and allocation of medical resources of different types of hospitals during the outbreak. In what follows, we investigate the elasticity of R_0^{FSH} with respect to the delay parameters τ_3 and τ_4 to identify which one has the most significant impact on R_0^{FSH} for system (2.9).

To investigate how R_0^{FSH} varies as a key parameter p changes and to obtain possible control strategies for the disease, we introduce the elasticity of R_0^{FSH} with respect to the parameter p [3, 24] as

$$\varepsilon^p = \frac{\partial R_0^{FSH}}{\partial p} \frac{p}{R_0^{FSH}},$$

which means that a change in the value of the parameter p leads to a change of ε^p in the quantity R_0^{FSH}.

From the expression of R_0^{FSH}, we discuss how changes in τ_3 and τ_4 affect R_0^{FSH} via the expressions

$$\varepsilon^{\tau_3} = \frac{\partial R_0^{FSH}}{\partial \tau_3} \frac{\tau_3}{R_0^{FSH}} = \frac{S^0 a \beta_2}{(1 + m\tau_1)(1 + m\tau_2) R_0^{FSH}} p_1 e^{-(r_m + m)\tau_3} \tau_3 \geq 0,$$

$$\varepsilon^{\tau_4} = \frac{\partial R_0^{FSH}}{\partial \tau_4} \frac{\tau_4}{R_0^{FSH}} = \frac{S^0 a \beta_2}{(1 + m\tau_1)(1 + m\tau_2) R_0^{FSH}} p_2 e^{-(d_s + m)\tau_4} \tau_4 \geq 0.$$

An increase in the value of either delay τ_3 or τ_4 thus leads to an increase in the value of R_0^{FSH}. Conversely, decreasing either delay can effectively decrease the reproductive number R_0^{FSH} which is beneficial to disease control. Notice that a decrease of τ_3 or τ_4 implies the reduction in the waiting time of patients for either type of hospitals.

Both expressions (ε^{τ_3} and ε^{τ_4}) depend on the average proportion of patients admitted (p_1 and p_2), the waiting time for admission (τ_3 and τ_4), and the removal rate of patients ($r_m + m$ and $d_s + m$). According to the actual status of the epidemic in Wuhan [49], it can be derived that $p_1 > p_2$, $\tau_3 < \tau_4$, and $r_m > d_s$. It is not easy to draw a general theoretical conclusion on which one of the parameters (τ_3 and τ_4) has a larger impact on R_0^{FSH} by directly comparing the values of ε^{τ_3} and ε^{τ_4}. However, it does provide a theoretical foundation for further numerical comparisons, which we present in section 7.

6.2. Relative contribution of the two types of hospitals DHs and FSHs. As stated in [5, 22], the construction and operation of the FSHs had a tremendous impact on curbing and eventually stopping the COVID-19 epidemic in China. As a comparison, how can we quantify the relative contribution of the two types of hospitals in the epidemic prevention and control?

Here, we perform a comparative study on the number of infections and deaths with or without FSHs as done in [22]. Besides, it is widely known that the waiting time for patients to be admitted largely depends on the adequacy of medical resources, including medical workers, the number of beds, protective equipment, and other resources.

The shorter the waiting time is, the more timely the corresponding hospitalization will be, which is more conducive to the control of the epidemic situation. Therefore, the time lag in our study also can be used to describe the timeliness and contribution of the hospital to a large extent. Recalling the expressions for R_0^{noFSH} and R_0^{FSH}, we see that accelerating the speed of patients entering the hospital has a positive effect on combating the spread of the epidemic. Combined with the analysis of the elasticity of R_0^{FSH}, we define a specific index K to quantify the relative contribution of the hospital,

$$K = \frac{\varepsilon^{\tau_3}}{\varepsilon^{\tau_4}} = \frac{p_1}{p_2} \frac{e^{-(r_m+m)\tau_3}}{e^{-(d_s+m)\tau_4}} \frac{\tau_3}{\tau_4},$$

which is jointly determined by the average proportions of patients admitted (p_1 and p_2), the waiting times for admission (τ_3 and τ_4), and the removal rates of patients ($r_m + m$ and $d_s + m$). In this expression, $\frac{p_1}{p_2} \frac{e^{-(r_m+m)\tau_3}}{e^{-(d_s+m)\tau_4}}$ represents the ratio of patients entering FSHs versus DHs, and $\frac{\tau_3}{\tau_4}$ is the ratio of the waiting time of patients to either hospitals. If $K = 1$, we have $\varepsilon^{\tau_3} = \varepsilon^{\tau_4}$, which implies that the impact of FSH resources on epidemic control is equal to that of DH resources; in other words, the contribution of these two hospitals is equivalent. If $K > 1$, we have $\varepsilon^{\tau_3} > \varepsilon^{\tau_4}$, and the FSH's contribution is greater than the DH's contribution. Otherwise, the DH's contribution is larger.

7. Parameter estimation and simulation. We estimate some model parameters and initial values by fitting the model to the infection data of Wuhan. Further, we explore how the epidemic or the spreading risk varies as some key parameters change. We also evaluate and compare the two types of hospitals to provide deeper insight for better understanding the possible control strategies.

Parameter estimation.
It is clear from the form of the proposed models that multiple parameters and initial values determine the dynamics of the epidemic. Some of parameter values could be

extracted from the literature (see Table 1), but others were not available. To obtain a set of more practical parameter values that captures the regional dynamics, we use the regional epidemiological data in Wuhan of China in 2020 as a case study. We collected some data of confirmed COVID-19 cases from the official website of Wuhan Municipal Health Commission (WMHC) [47].

Data information aggregates the cumulative numbers of reported confirmed, cured, and death cases from January 23 to February 23, 2020, and the cumulative number of beds in FSHs from February 5 to February 23, 2020. The period of January 23 to February 23, 2020, is chosen to emphasize the role played by FSHs: the first group of beds in FSHs was put into operation on February 5, 2020 and even if new beds were added thereafter, no vacant bed became available until February 23, 2020.

It is worth pointing out that, in Wuhan, the daily newly confirmed cases increased dramatically on February 12, 2020. Besides the possibile cases developed following the course of spreading, the other main reason might be the change in the definition of confirmed cases, which includes clinically confirmed cases [8, 45]. In literature, researchers have two different ways to implement Wuhan data into their models. One is to estimate the parameters directly from data without reconstructing the data [11]; the other is to smooth the data by using the averaging method or other techniques to process the data before use [52]. In this study, we choose to respect the data as it is without editing the data. In data fitting, we are not solely relying on this set of data of confirmed cases. Instead, we also collected three other sets of data (accumulative death, accumulative recovery cases, and number of Fangcang hospital beds), so we used four different sets of data simultaneously to do data fitting to increase the accuracy in our parameter estimation.

Based on the real epidemiological time series and two-stage models, we inferred most of the uncertain parameters and initial values by applying the Markov chain Monte Carlo (MCMC) method [12]. The adaptive Metropolis–Hastings algorithm was applied to carry out the MCMC procedure with 100,000 iterations and a burn-in of the first 50,000 iterations. The estimated mean values are shown in Tables 1 and 2. The fitting results are very good (normalized mean square error $= 0.9848$) and presented in Figure 2.

Effect of FSHs. To emphasize the role of FSHs, we examine the changes in the cumulative cases and deaths over time with and without FSHs. From Figure 3, we find that the cumulative numbers of infections and deaths without FSHs will reach 845,500 and 49,230, respectively, which are values 17 and 24 times those with FSHs on February 23, 2020.

Effect of patients' admission speed into the hospitals. Our models are designed to explore the impacts of patients' admission speed into the hospital on the COVID-19 epidemic. Therefore, we highlight the effects of parameters τ_3 and τ_4 which are the average waiting times of patient admission into the hospital and keys in determining the hospital admission rate to DHs or the centralized isolation admission rate to FSHs. We made a set of contour plots of the peak time of infected cases (Figure 4 (upper-left)), the peak time (upper-right), the cumulative number of infections (lower-left), and the cumulative number of deaths (lower-right) in terms of τ_3 and τ_4 to visualize their variation. Figure 4 shows that, with decreases in the values of τ_3 and τ_4, the peak time is advanced, the peak size is reduced, and the final sizes of infections and deaths are decreased, illustrating that shortening the admission time of patients into hospitals does reduce the severity of the epidemic.
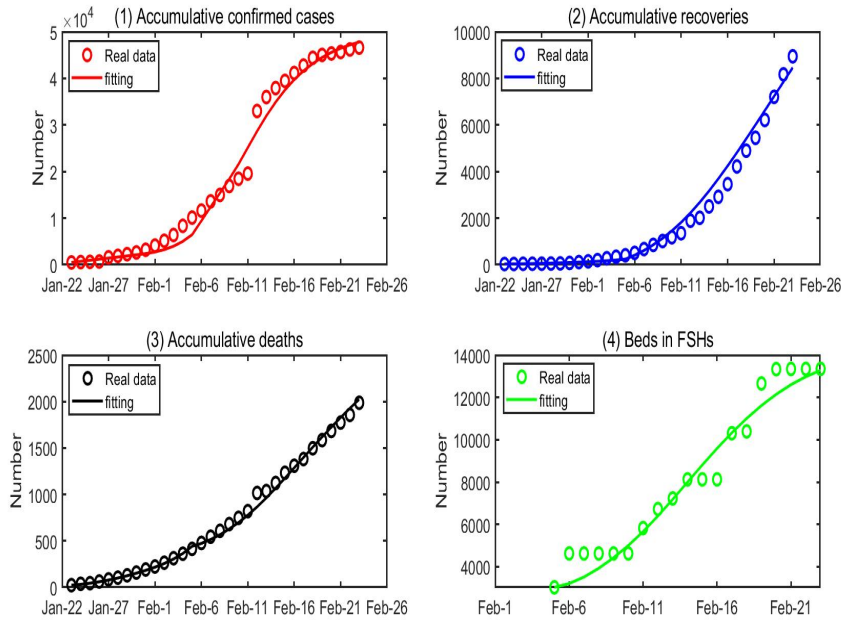
FIG. 2. *Fitting for the data of COVID-19 in Wuhan, China, February 5–23, 2020: plotting (1) for the cumulative number of confirmed cases, (2) for the cumulative number of recoveries, (3) for the cumulative number of deaths, and (4) for the number of beds in FSHs. The circle represents real data, and a solid curve is the best fitting from the model to the data. The data source is from WMHC [47].*
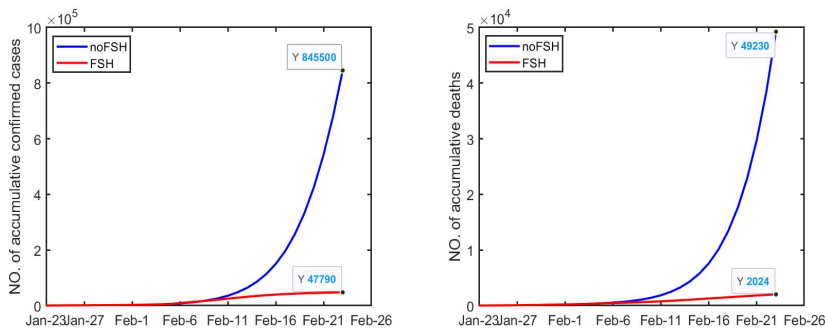
FIG. 3. *Impact of the FSHs on the cumulative number of infections and deaths over time.*

We also plot the maximum occupancy of beds in FSHs and the arrival times of maximum occupancy (see Figure 5). These plots show that both the maximum occupancy of beds in FSHs and the arrival times increase as τ_3 and τ_4 increase. Besides, both figures in Figure 5 show that these two quantities are more sensitive to τ_3 than τ_4. If τ_3 is increased by 2 days and $\tau_4 = 4.17$ days, the arrival time is deferred by two days, and the maximum occupancy of beds is increased by 200.

Elasticity of R_0^{FSH}. According to the theoretical analysis in section 3, the basic reproduction number R_0 plays a significant role in determining the persistence and
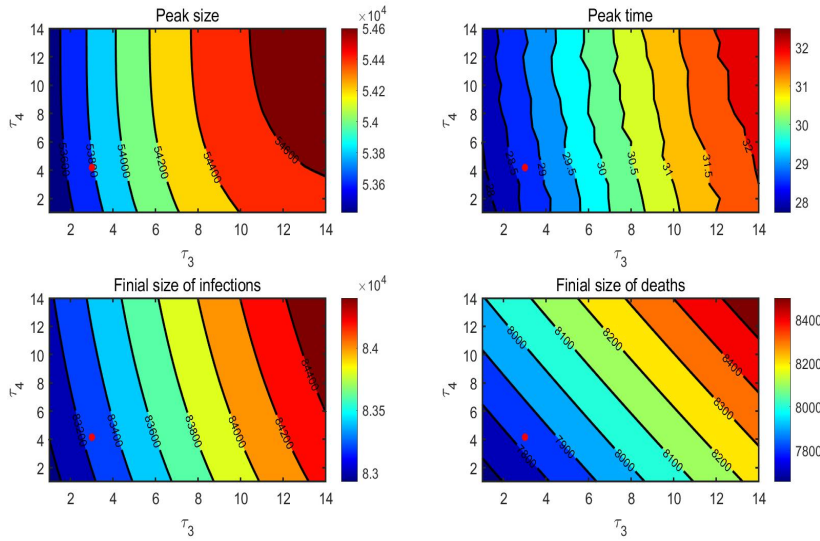
FIG. 4. *Contour plots of epidemic indicators including the peak size, peak time, and cumulative numbers of confirmed cases and deaths with respect to τ_3 and τ_4. The star represents the position of (τ_3, τ_4) estimated by fitting our model to the epidemiological data from Wuhan.*
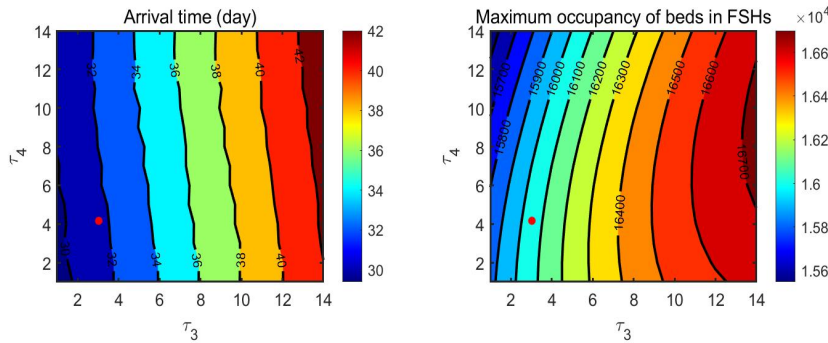
FIG. 5. *Contour plots of maximum occupancy of beds in FSHs and the arrival times in terms of τ_3 and τ_4. The star represents the position of (τ_3, τ_4) estimated by fitting our model to the epidemiological data from Wuhan.*

eradication of the disease. By fitting the model to the real data of Wuhan, we estimate the basic reproduction number of two systems (2.8) and (2.9) as $R_0^{noFSH} = 6.7742$ (95% confidence interval (CI) %: 5.9463–7.5299) and $R_0^{FSH} = 0.1739$ (95%CI: 0.1608–0.1890), respectively. We also plot the variations of the elasticity of R_0^{FSH} with respect to τ_3 and τ_4 in Figure 6. This plot reveals that delay τ_3 has a higher impact on R_0^{FSH} than τ_4. That means the influence of the waiting time to FSHs on the epidemic control is greater than the waiting time to DHs.

Relative contribution of the hospital. For the Wuhan epidemic, the estimated value of K is around 3 (see the red star in Figure 7) which is greater than 1. That means that the FSHs play a relatively larger role than the DHs in combating the COVID-19 epidemic in Wuhan.
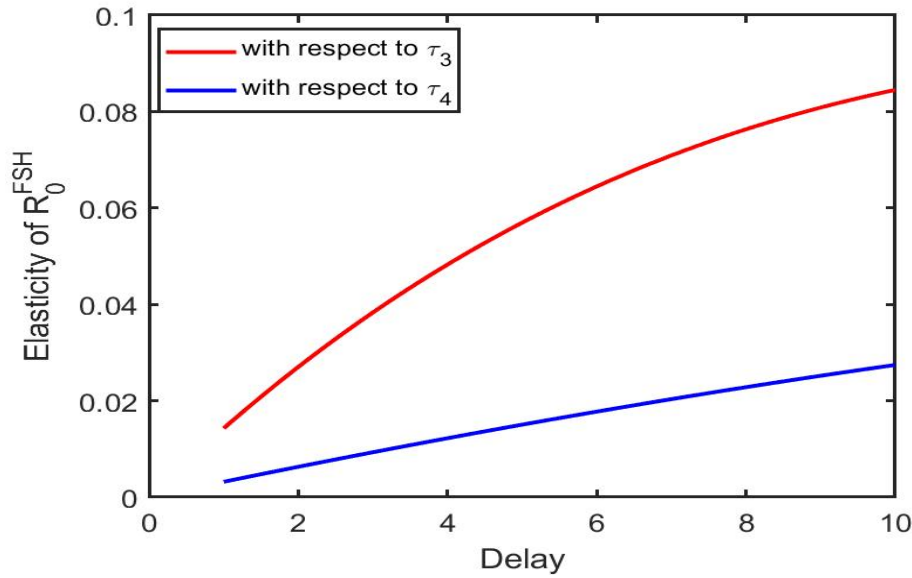
FIG. 6. *Variations of the elasticity of R_0^{FSH} with respect to τ_3 and τ_4, respectively.*
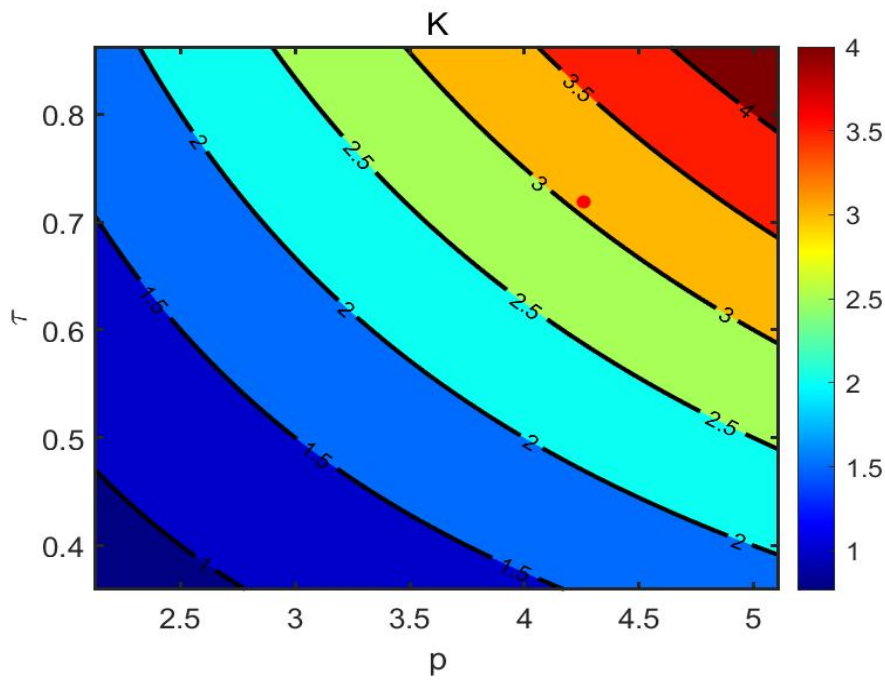
FIG. 7. *Contour plots of K with respect to p and τ, where $p = \frac{p_1}{p_2}$ and $\tau = \frac{\tau_3}{\tau_4} \frac{e^{-(r_m+m)\tau_3}}{e^{-(d_s+m)\tau_4}}$. The red star represents the position of (p, τ) estimated by fitting our model to the epidemiological data from Wuhan.*

When quantifying the relative contributions of these two types of hospitals in disease control, it follows from the definitions of the elasticity of R_0^{FSH} and the relative contribution index K that these two indexes played a mutually equivalent role. However, the expression of the relative contribution index is simpler and convenient in the application. Its numerical result is more intuitive and easy to be understand. Through the above numerical analysis, we can obtain that, no matter which measure is used to compare the variation of the epidemiological indicators (final size, peak size, or peak time etc.) with or without FSHs, or to compare the elasticity of R_0^{FSH} with respect to the admission speeds of different hospitals, or our self-defined relative contribution index, FSHs indeed play a significant role in the COVID-19 control in China, which supports the result obtained in Li et al. [22].

8. Discussion and conclusion. The role of FSHs in the pandemic control in Wuhan has been discussed in [5, 22]. The acceptance speed of patients into either hospital, once confirmed, is also an important index to reflect the efficiency of the current public health system in dealing with the control of the disease. In this paper, we used Wuhan as a case study and proposed a delayed dynamical transmission model of COVID-19. We investigated in-depth the impact of accepting speed of patients on disease control. We defined a relative contribution index K to conduct some quantitative analysis on the contributions of both hospitals during the control process of the pandemic in Wuhan.

Unlike [22], we used delayed differential equations with delays representing the waiting time of a confirmed patient for hospitalization (with τ_3 the waiting time of mildly infected patients for FSHs and τ_4 the waiting time of severely infected patients for DHs). Our model also shows the significant roles FSHs played in endemic control. In particular, our result indicates that FSHs played a relatively even larger contribution in mitigating the diseases in Wuhan than DHs in the sense that they efficiently reduced the potential further infections caused by the mildly infected patients staying outside of FSHs. Hence, it greatly reduced the magnitude of the pandemic which could be potentially amplified without the use of FSHs (see Figure 3), and also reduced the time course needed for the public health system to combat a disease such as in Wuhan which successfully controlled the diseases within two months of its outbreak compared to the still ongoing pandemic in lots of other countries like the United States and the United Kingdom.

The successful experience in Wuhan and our study both suggest that countries which are still suffering from the pandemic of COVID-19 may consider incorporating FSHs into their control system. For example, some countries modified public libraries or cruise ships and used them to centrally isolate mildly infected patients [5, 6]. If conditions permit, building FSHs or some other similar large area that can offer central isolation equipped with health care providers can efficiently cut the spreading routes from mildly infected patients to susceptible people and also speed up the recovery process of those mildly infected patients which in turn shortens the control process of the diseases.

Another conclusion that can be drawn from our analysis is that the faster all cases are traced, tested, and hospitalized (or isolated), the harder it is for the virus to spread, and thus we benefit to contain the contagion. The five "early" intervention strategies from the experience in Wuhan including early detection, early report, early testing, early isolation, and early treatment proved to be efficient in mitigating the pandemic. From the patient's point view, these five "early measures" can help identify the infected patients on time and give them necessary treatment and reduce their

death rate. On the other hand, the early isolation of hospitalized patients in places like FSHs can cut off the contact of infected patients with other susceptibles so that the "source of the virus" (i.e., the infected patients) is under control. Controlling the "source of the virus" greatly reduces the massive spread of the virus within the healthy group of people and protects them against infections.

REFERENCES

[1] A. Abdelrazec, J. Belair, C. Shan, and H. Zhu, *Modeling the spread and control of dengue with limited public health resources*, Math. Biosci., 271 (2016), pp. 135–145.

[2] The Straits Times, *Lessons from China's Successful Battle With Covid-19: China Daily*, https://www.straitstimes.com/asia/lessons-from-chinas-successful-battle-with-covid-19-china-daily (17 March 2020).

[3] N. Bai, C. Song, and R. Xu, *Mathematical analysis and application of a cholera transmission model with waning vaccine-induced immunity*, Nonlinear Anal. Real World Appl., 58 (2021), 103232, https://doi.org/10.1016/j.nonrwa.2020.103232.

[4] CCTV News, *The conversion rate from mild to severe was 2%−5%, 2020*, http://news.cctv.com/2020/03/24/ARTI8hYjp1pdaaKnm7wE1zEN200324.shtml (24 March 2020).

[5] S. Chen, Z. Zhang, J. Yang, J. Wang, X. Zhai, T. Bärnighausen, and C. Wang, *Fangcang shelter hospitals: A novel concept for responding to public health emergencies*, The Lancet, 58 (2020), pp. 1305–1314, https://doi.org/10.1016/S0140-6736(20)30744-3.

[6] W. Chen, *The Shelter Hospital Can Be Regarded as a "Cabin" on Noah's Ark. Its Original Intention Is to Achieve "All Accounts Receivable"*, https://china.huanqiu.com/article/9CaKrnKpdvC (5 February 2020).

[7] H. Ellyatt, *Third Covid Wave Hits Europe: Lockdowns Imposed and Vaccines Remain a Problem*, https://www.cnbc.com/2021/03/22/third-covid-wave-hits-europe-france-germany-eye-more-lockdowns.html (7 April 2021).

[8] The China National Health Commission, *Diagnosis and Treatment Protocol for COVID-19 (Trial Version 5)*, http://www.nhc.gov.cn/yzygj/s7653p/202002/d4b895337e19445f8d728fcaf1e3e13a.shtml (8 February 2020).

[9] L. Dell'Anna, *Solvable delay model for epidemic spreading: The case of Covid-19 in Italy*, Sci. Rep., 10 (2020), 15763, https://doi.org/10.1038/s41598-020-72529-y.

[10] S. Eikenberry, M. Mancuso, and E. Iboi, *To mask or not to mask: Modeling the potential for face mask use by the general public to curtail the COVID-19 pandemic*, Infect. Dis. Model., 5 (2020), pp. 293–308.

[11] S. Feng, J. Zhang, J. Li, X. Luo, H. Zhu, M. Y. Li, and Z. Jin, *The impact of quarantine and medical resources on the control of COVID-19 in Wuhan based on a household model*, Bull. Math. Biol., 84 (2022), 47, https://doi.org/10.1007/s11538-021-00989-y.

[12] H. Haario, M. Laine, A. Mira, and E. Saksman, *Dram: Efficient adaptive MCMC*, Stat. Comput., 16 (2006), pp. 339–354, https://doi.org/10.1007/s11222-006-9438-0.

[13] J. K. Hale and S. M. Verduyn Lunel, *Introduction to Functional Differential Equations*, 1st ed., Springer, New York, 1993.

[14] Harvard Health Publishing, *Treatments for COVID-19: What Helps, What Doesn't, and What's in the Pipeline*, https://www.health.harvard.edu/diseases-and-conditions/treatments-for-covid-19 (18 May 2022).

[15] D. Yetman, *How Ventilators Can Save the Lives of People With COVID-19*, https://www.healthline.com/health/ventilator-covid#with-covid-19 (15 March 2021).

[16] C. Huang, Y. Wang, X. Li, L. Ren, J. Zhao, Y. Hu, L. Zhang, G. Fan, et al., *Clinical Features of Patients Infected with 2019 Novel Coronavirus in Wuhan, China*, The Lancet, 395 (2020), pp. 497–506, https://doi.org/10.1016/S0140-6736(20)30183-5.

[17] R. Jing, R. R. Vunnam, Y. Yang, A. Karevoll, and S. R. Vunnam, *Current status of treatment options, clinical trials, and vaccine development for SARS-CoV-2 infection*, J. Pure Appl. Microbiol., 14 (2020), pp. 733–740, https://doi.org/10.22207/JPAM.14.SPL1.10.

[18] Johns Hopkins Medicine, *New Variants of Coronavirus: What You Should Know*, https://www.hopkinsmedicine.org/health/conditions-and-diseases/coronavirus/a-new-strain-of-coronavirus-what-you-should-know (29 April 2021).

[19] M. Kretzschmar, G. Rozhnova, M. Bootsma, M. van Boven, J. van de Wijgert, and M. Bonten, *Impact of delays on effectiveness of contact tracing strategies for COVID-19: A modelling study*, Lancet Public Health, 5 (2020), pp. e452–e459, https://doi.org/10.1016/S2468-2667(20)30157-2.

[20] Y. KUANG, *Delay Differential Equations: With Applications in Population Dynamics*, Academic Press, New York, 1993.

[21] F. LI, J. LIU, AND X.-Q. ZHAO, *A West Nile virus model with vertical transmission and periodic time delays*, J. Nonlinear Sci., 20 (2020), pp. 449–486, https://doi.org/10.1007/s00332-019-09579-8.

[22] J. LI, P. YUAN, J. HEFFERNAN, T. ZHENG, N. OGDEN, B. SANDER, J. LI, J. BÉLAIR, ET AL., *Fangcang shelter hospitals during the COVID-19 epidemic, Wuhan, China*, Bull. World Health Organ., 98 (2021), pp. 830–841D, https://doi.org/10.2471/BLT.20.258152.

[23] Z. LIU, P. MAGAL, O. SEYDI, AND G. WEBB, *A COVID-19 epidemic model with latency period*, Infect. Dis. Model., 5 (2020), pp. 323–337, https://doi.org/10.1016/j.idm.2020.03.003.

[24] M. MARTCHEVA, *An Introduction to Mathematical Epidemiology*, 1st ed., Springer, New York, 2015.

[25] D. CYRANOSKI AND A. SILVER, *Wuhan Scientists: What It's Like to Be on Lockdown*, https://www.nature.com/articles/d41586-020-00191-5 (24 January 2020).

[26] E. FENG AND A. CHENG, '*We No Longer Wish for Much': People of Wuhan Share Stories of Loss and Survival*, https://www.npr.org/2020/06/26/882018866/we-no-longer-wish-for-much-people-of-wuhan-share-stories-of-loss-and-survival (26 June 2020).

[27] REUTERS STAFF, *Toronto Cancels In-Person Schooling as Canada Deals with Variant-Driven Wave of Coronavirus*, https://www.reuters.com/article/us-health-coronavirus-canada/canada-is-facing-very-serious-third-wave-of-covid-19-pandemic-pm-trudeau-idUSKBN2BT256 (6 April 2021).

[28] X. RONG, Y. LIU, H. CHU, AND M. FAN, *Effect of delay in diagnosis on transmission of COVID-19*, Math. Biosci. Eng., 17 (2020), pp. 2725–2740, https://doi.org/10.3934/mbe.2020149.

[29] C. SHAN, Y. YI, AND H. ZHU, *Nilpotent singularities and dynamics in an SIR type of compartmental model with hospital resources*, J. Differential Equations, 260 (2016), pp. 4339–4365.

[30] C. SHAN AND H. ZHU, *Bifurcations and complex dynamics of an SIR model with the impact of the number of hospital beds*, J. Differential Equations, 257 (2014), pp. 1662–1688.

[31] H. SMITH, *Monotone Dynamical Systems: An Introduction to the Theory of Competitive and Cooperative Systems*, 1st ed., American Mathematical Society, Providence, RI, 1995.

[32] SNOHOMISH HEALTH DISTRICT, *Non-Pharmaceutical Interventions (NPI Coronavirus (COVID-1029))*, http://www.snohd.org/DocumentCenter/View/3420/Poster_from_NPI_85x11_2020_03_02_LML?bidId= (13 January 2023).

[33] K. SOLTESZ, F. GUSTAFSSON, T. TIMPKA, J. JALDÉN, C. JIDLING, A. HEIMERSON, T. B. SCHÖN, A. SPRECO, ET AL., *The effect of interventions on COVID-19*, Nature, 588 (2020), pp. 26–28, https://doi.org/10.1038/s41586-020-3025-y.

[34] HEALTH, PHARMA & MEDTECH, STATE OF HEALTH, STATISTA, *Number of Coronavirus (COVID-19) Cases Worldwide as of January 9, 2023, by Country or Territory*, https://www.statista.com/statistics/1043366/novel-coronavirus-2019ncov-cases-worldwide-by-country/ (13 January 2023).

[35] HEALTH, PHARMA & MEDTECH, HEALTH PROFESSIONALS & HOSPITALS, STATISTA, *Number of New Hospital Beds to be Added in the Designated Hospitals After the Coronavirus COVID-19 Outbreak in Wuhan, China as of February 2, 2020*, https://www.statista.com/statistics/1095434/china-changes-in-the-number-of-hospital-beds-in-designated-hospitals-after-coronavirus-outbreak-in-wuhan/ (7 April 2021).

[36] H. THIEME, *Global asymptotic stability in epidemic models,* in Equadiff 82, H. W. Knobloch and K. Schmitt, eds., Lecture Notes in Math. 1017, Springer, Berlin, 1983, pp. 608–615.

[37] H. R. THIEME, *Spectral bound and reproduction number for infinite-dimensional population structure and time heterogeneity*, SIAM J. Appl. Math., 70 (2009), pp. 188–211, https://doi.org/10.1137/080732870.

[38] WORLD HEALTH ORGANIZATION, *WHO's COVID-19 Response*, https://www.who.int/emergencies/diseases/novel-coronavirus-2019/interactive-timeline#event-71 (7 April 2021).

[39] C. WANG, P. W. HORBY, F. G. HAYDEN, AND G. F. GAO, *A novel coronavirus outbreak of global health concern*, The Lancet, 395 (2020), pp. 470–473, https://doi.org/10.1016/S0140-6736(20)30185-9.

[40] D. WANG, B. HU, C. HU, F. ZHU, X. LIU, J. ZHANG, B. WANG, H. XIANG, ET AL., *Clinical characteristics of 138 hospitalized patients with 2019 novel coronavirus-infected pneumonia in Wuhan, China*, JAMA, 323 (2020), pp. 1061–1069, https://doi.org/10.1001/jama.2020.1585.

[41] World Health Organization, *Coronavirus (COVID-*19*) Dashboard*, https://covid19.who.int/ (6 April 2021).

[42] World Health Organization, *Naming the Coronavirus Disease (COVID-*19*) and the Virus That Causes It*, https://www.who.int/emergencies/diseases/novel-coronavirus-2019/technical-guidance/naming-the-coronavirus-disease-(covid-2019)-and-the-virus-that-causes-it (11 February 2020).

[43] Worldometer, *Worldometer Coronavirus Updates*, https://www.worldometers.info/coronavirus/?utm_campaign=homeAdUOA?Si_23countries (6 April 2021).

[44] Z. Wu and J. M. McGoogan, *Characteristics of and important lessons from the coronavirus disease* 2019 *(COVID-*19*) outbreak in China: Summary of a report of* 72314 *cases from the Chinese center for disease control and prevention*, JAMA, 323 (2020), pp. 1239–1242, https://doi.org/10.1001/jama.2020.2648.

[45] Wuhan Municipal Health Commission, *Epidemic Situation of Covid-19 in Hubei Province on February 12, 2020*, http://wjw.wuhan.gov.cn/ztzl_28/fk/yqtb/202004/t20200430_1197352.shtml (13 January 2023).

[46] Wuhan Municipal Bureau of Statistics, *Statistical Bulletin of Wuhan National Economic and Social Development in 2019*, http://tjj.wuhan.gov.cn/tjfw/tjgb/202004/t20200429_1191417.shtml (18 April 2021).

[47] Wuhan Municipal Health Commission, *Wuhan Municipal Health Commission (WMHC) Website*, http://wjw.wuhan.gov.cn/gsgg/ (1 February 2021).

[48] Wuhan Municipal Health Commission, *Daily Report, 2020*, http://wjw.wuhan.gov.cn/ztzl_28/fk/yqtb/index_28.shtml (18 April 2021).

[49] Y. Zhang, *The epidemiological characteristics of an outbreak of* 2019 *novel coronavirus diseases (COVID-*19*) in China*, Chin. J. Epidemiol., 41 (2020), pp. 145–151.

[50] X.-Q. Zhao, *Basic reproduction ratios for periodic compartmental models with time delay*, J. Dynam. Differential Equations, 29 (2017), pp. 67–82, https://doi.org/10.1007/s10884-015-9425-2.

[51] F. Zhou, T. Yu, R. Du, G. Fan, Y. Liu, Z. Liu, J. Xiang, Y. Wang, et al., *Clinical course and risk factors for mortality of adult inpatients with COVID-*19 *in Wuhan, China: A retrospective cohort study*, The Lancet, 395 (2020), pp. 1054–1062.

[52] W. Zhou, A. Wang, X. Wang, R. Cheke, Y. Xiao, and S. Tang, *Impact of hospital bed shortages on the containment of COVID-*19 *in Wuhan*, Int. J. Environ. Res. Public Health, 17 (2020), 8560, https://doi.org/10.3390/ijerph17228560.